Revista de Chimie
https://revistadechimie.ro
https://doi.org/10.37358/Rev.Chim.1949

Preparation of Vermiculite-based Ni-phyllosilicate for Dry Reforming of Methane

XIAOFENG ZHU[1,2], TENG ZHAO[1,2], YUFAN HUANG[1,2], ZIJUN WANG[1,2*]
[1] School of Chemistry and Chemical Engineering, Shihezi University, Shihezi, Xinjiang 832003, PR China
[2] Key Laboratory for Green Processing of Chemical Engineering of Xinjiang Bingtuan/Engineering Research Center of Materials-Oriented Chemical Engineering of Xinjiang Bingtuan, Shihezi, Xinjiang 832003, PR China

Abstract: *Layered porous SiO_2 (V-SiO_2) was designed and prepared from vermiculite by expansion-acidification method, and then used as a catalyst support to prepare Ni/V-SiO_2 for dry reforming of methane. It is well known that sintering and carbon deposition of metal particles are two main problems in deactivation of nickel-based catalysts for methane dry reforming. It is reported that strong metal support interaction is a possible solution. Here, a Ni/V-SiO_2-H catalyst derived from Ni-phyllosilicate was developed, and compared with the catalyst Ni/V-SiO_2-IM by impregnation method. The results showed that the Ni/V-SiO_2-H catalyst had high catalytic activity and stability, and the CH_4 conversion reached 71.7% at 700 °C. The reason is that on the one hand, the active metal particles in the catalyst are small (8.3 nm) and relatively evenly dispersed; on the other hand, the catalyst has strong metal support interaction, which improves the anti sintering ability of the catalyst and affects the catalytic activity. It is considered that V-SiO_2 as a catalyst support for the preparation of Ni-phyllosilicate may have wide application.*

Keywords*: vermiculite, dry reforming, Ni-phyllosilicate, CO_2*

1. Introduction

In recent decades, the extensive use of fossil fuels has emitted a large number of greenhouse gases into the atmosphere, which has seriously affected the earth's climate and the global ecological environment. At the same time, although considerable efforts have been made to reduce greenhouse gas emissions, there is no effective treatment of greenhouse gases in practical application worldwide [1-5]. Dry reforming of methane (DRM), as shown in Eq. (1), which involves the simultaneous consumption of two greenhouse gases, *i.e.*, methane and carbon dioxide, has been widely concerned. It produces syngas with a H_2/CO ratio equal to 1, which is suitable for the synthesis of liquid fuel [6-7]. Unfortunately, there are some difficult issues that lead to DRM not being widely processed in industry so far. According to the thermodynamics of DRM, it must be carried out at high temperature, which leads to catalyst deactivation due to sintering of active metal [8-9]. In addition, methane decomposition Eq. (2) and carbon monoxide disproportionation Eq. (3) are also the main reasons for deactivation [10-11]. Therefore, how to choose the right catalyst has gradually become the focus of researchers, which is still a challenge up to now [12].

$$CH_4 + CO_2 \rightarrow 2H_2 + 2CO \; \Delta H^{\circ}_{298} = +247 \; kJ \; mol^{-1} \quad (1)$$

$$CH_4 \rightarrow C + 2H_2 \; \Delta H^{\circ}_{298} = +75 \; kJ \; mol^{-1} \quad (2)$$

$$2CO \rightarrow C + CO_2 \; \Delta H^{\circ}_{298} = -172 \; kJ \; mol^{-1} \quad (3)$$

In general, dry reforming of methane is carried out on metal catalysts. Although noble metal catalysts, such as Rh [13], Pt [14], and Pd [15], exhibit excellent catalytic activity and stability, the high cost and limited reserves of noble metals make it difficult to be widely used in commercial applications [16]. Nickel-based catalysts are supposed to be the best choice based on their low cost and high activity in dry reforming [17]. Unfortunately, under dry reforming conditions, nickel catalysts are usually easy

**email: wzj_tea@shzu.edu.cn*

to sinter to form nickel clusters, and it is easier to coke due to excessively high reaction temperature and side reactions, resulting in rapid deactivation [18-19]. Therefore, other methods are needed to overcome these shortcomings.

Support plays a key role in the design of catalyst. In order to develop stable nickel-based catalysts, researchers have made many attempts, using different supports, such as Al_2O_3, MgO, CaO, ZrO_2, rare earth metal oxides, CeO_2, La_2O_3 and so on [20]. Some supports, such as MgO and CaO, have basic sites, which lead to lower carbon deposition rate in dry reforming methane [21]. Except above mentioned support, SiO_2 has a high specific surface area and good thermal stability, and has been successfully and widely applied in dry reforming methane.

Moreover, the properties of the support are also important to the catalytic performance. It is believed that a higher specific surface area is conducive to obtain metal particles with uniform dispersion and smaller particle size, so as to improve the activity and stability of the catalyst [22]. Large specific surface area SiO_2, including SBA-15, MCM-41, etc., has higher cost and harsher preparation conditions. While SiO_2 derived from clay may be potential, with the advantages of large specific surface area, porous, cheap and easy to obtain [23]. Li et al. [24] used layered clay as a raw material to prepare a two-dimensional porous SiO_2 nanomesh (2D-VMT-SiO_2) by a mixed acid etching method, and successfully applied to the catalyst support for the methanation of carbon monoxide. Compared with Ni/MCM-41, Ni/2D-VMT-SiO_2 exhibits superior catalytic activity. It can be considered that clay-derived SiO_2 has application prospects as a catalyst support.

Nickel supported on SiO_2 is a common catalyst. It is well known that active metals are usually introduced to the surface of the support by wet impregnation method. However, the metal-support interaction caused by impregnation is usually too weak to prevent nickel from sintering at high temperature [25]. Due to its unique structure and properties, Ni-phyllosilicate provides strong metal-support interaction, which is suitable for dry reforming of methane. After high temperature reduction, the metal nanoparticles of the catalyst are tiny and well dispersed [26]. Zhang et al. [27] reported the preparation of Ni-phyllosilicate by facile template-free hydrothermal method for dry reforming of methane. This strong interaction stabilized the Ni species on SiO_2, and the phenomenon of metal sintering and carbon deposition was hardly observed during the test.

In this paper, layered clay vermiculite (VMT) was used as raw material to obtain support vermiculite derived SiO_2 (V-SiO_2), and Ni phyllosilicate was synthesized by a simple hydrothermal process. For comparison, a catalyst was prepared by impregnation. The catalyst was obtained and then tested in dry reforming of methane. Brunauer Emmett Teller (BET), X-Ray Diffraction (XRD), X-ray Photoelectron Spectroscopy (XPS), H_2-Temperature-Programmed Reduction (H_2-TPR), Transmission Electron Microscopy (TEM) and Thermogravimetric Analysis (TGA) were employed to characterize the catalyst, so as to verify the effect of catalyst structure on the catalyst performance.

2. Materials and methods

2.1. Catalyst preparation

Layered porous SiO_2 (V-SiO_2) derived from vermiculite was prepared by acid leaching method, and the preparation method was referred to the literature [28]. Raw vermiculite and H_2O_2 were put into a beaker, the mixture was heated at 80°C for 1 h, and then dried in a 700 W microwave oven for 5 min. The dried expanded multilayer vermiculite was ground and poured into 2 mol/L hydrochloric acid solution for 12 h at 50°C to obtain the catalyst support V-SiO_2. The chemical composition was shown in Table 1. The obtained silica powder was dispersed in deionized water at room temperature, and $Ni(NO_3)_2 \cdot 6H_2O$ was added and dissolved. Then, ammonia was added dropwise until the *p*H of the solution reached 10, stirring vigorously for 30 min, and the resulting mixture was transferred to an autoclave at 120°C for 24 h. After cooling to room temperature, the product was separated and washed several times by centrifugation, then dried at 100°C for 12 h. Finally, the powder was calcined at 700°C for 4 h with a heating rate of 2°C/min. The resulting catalyst is labeled Ni/V-SiO_2-H, where the Ni loading is 10 wt.%.

For comparison, the catalysts were prepared by wet impregnation method labeled as Ni/V-SiO_2-IM. Among them, the Ni loading, drying and calcination conditions are the same as above.

Table 1. The main chemical composition of samples (wt.%)

Sample	SiO_2	MgO	Al_2O_3	K_2O	Fe_2O_3
vermiculite	42.87	24.14	16.26	5.82	4.93
V-SiO_2	97.07	0.92	0.51	0.53	0.35

2.2. Catalytic performance

The catalyst activity of DRM was measured in a fixed bed reactor (internal diameter of 6 mm, length of 400 mm), and 100 mg of catalyst was filled in a quartz tube lined with quartz sand, which was located in the center of the fixed bed. Before the DRM test, the catalyst was reduced at 700°C for 2 h at 50 mL/min, 10% H_2/Ar atmosphere. After the reaction, the temperature was kept unchanged, and feed gas with a molar ratio of 1:1:1 of N_2, CH_4 and CO_2 was introduced with a total flow rate of 30 mL/min, corresponding to a gas hourly space velocity of 18,000 mL h^{-1} g_{cat}^{-1}. The gas at the outlet was analyzed online through a gas chromatograph (GC, Fuli 9790) equipped with TCD, using Ar as a carrier gas. The conversion rate of CH_4 and CO_2 is calculated by Eqs. (4) and (5), where *n* is the number of moles and subscripts *in* and *out* indicate the inlet and outlet.

$$X_{CH_4}\% = \frac{n_{CH_4,in} - n_{CH_4,out}}{n_{CH_4,in}} \quad (4)$$

$$X_{CO_2}\% = \frac{n_{CO_2,in} - n_{CO_2,out}}{n_{CO_2,in}} \quad (5)$$

2.3. Catalytic characterization

N_2 Adsorption-Desorption. N_2 adsorption-desorption isotherms were investigated in the presence of liquid nitrogen with temperature of -196°C using a Micromeritics ASAP 2020 apparatus. Samples were degassed at 150°C for 12 h before tests. The specific surface areas were calculated by the BET method. The average pore diameters and pore volumes were obtained by the BJH method.

X-Ray Diffraction (XRD). XRD patterns were performed on a Bruker D8 X-ray diffractometer with Cu Kα radiation (k = 1.5406 Å, 40 kV, 30 mA). The data were collected in the range of 10-90°, with a scanning rate of 5°/min.

X-ray Photoelectron Spectroscopy (XPS). XPS measurements of the prepared samples were obtained with a PHI 5000 Versa Probe spectrometer, in which the C1s line at 284.8 eV binding energy was referenced.

H_2-Temperature Programmed Reduction (H_2-TPR). The reduction performance of the catalyst was studied using the H_2 temperature programmed reduction (H_2-TPR) in the instrument Micromeritics ASAP 2920, a thermal conductivity detector (TCD) was used to monitor H_2 consumption in real time. Before the test, first 0.1 g sample was pre-treated at 300°C for 1h under He flow (30 mL/min). After cooling to room temperature, the test was carried out from 100°C to 800°C at a heating rate of 10°C/min with 10% H_2/Ar (50 mL/min).

Transmission Electron Microscopy (TEM). The powder samples were deposited on a copper grid covered by a porous carbon film for TEM experiments on a FEI Tecnai G F20 high resolution field emission transmission electron microscope.

Thermogravimetric Analysis (TGA). TGA was performed with a TGA instrument (SDT Q600) in air atmosphere. In this experiment, samples (20 mg) were heated from 30 to 900°C with a heating rate of 10°C/min.

3. Results and discussions

3.1. N_2 adsorption-desorption analysis

Table 2. Textural parameters of V-SiO_2 and Ni/V-SiO_2 catalysts.

Sample	S_{BET} (m^2 g^{-1})	Pore volume (cm^3 g^{-1})
V-SiO_2	630.7	0.46
Ni/V-SiO_2-H	139.3	0.24
Ni/V-SiO_2-IM	287.8	0.26

The nitrogen adsorption-desorption results of the catalyst Ni/V-SiO_2 and the support are shown in Figure 1, and the texture parameters are summarized in Table 2. As shown in Table 2, the introduction of metallic nickel by impregnation or hydrothermal method significantly reduces the specific surface area and pore volume of the support. This result shows that the introduction of nickel occupies the surface of the support or blocks the pores to a certain extent [29]. However, there is no obvious change in the morphology from the nitrogen adsorption-desorption curve, and it is possible that the main structure of the support was not destroyed during the preparation of the catalyst. In addition, the specific surface area of Ni/V-SiO_2-H is much smaller than the specific surface area of Ni/V-SiO_2-IM, which may infer that occupied more pores of the support. In other words, the Ni particles of the catalyst Ni/V-SiO_2-H may be more uniformly distributed.

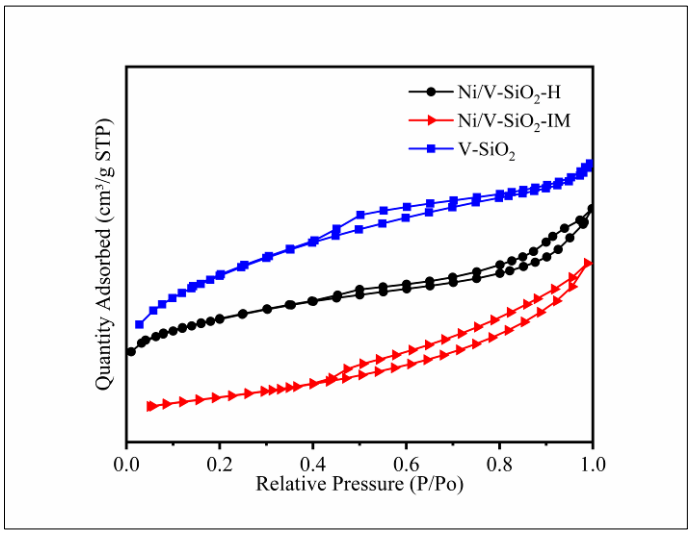

Figure 1. N_2 adsorption/desorption isotherms for calcined V-SiO_2 and Ni/V-SiO_2 samples

3.2. XRD and analysis of calcined and reduced catalysts

The XRD images of the calcined catalyst are shown in Figure 2. For Ni/V-SiO_2-IM, there is an obvious diffraction peak at $2\theta = 37.2°$, corresponding to the (111) crystal surface of NiO. In contrast, there is no diffraction peak about NiO in the pattern of Ni/V-SiO_2-H, but there is a weak diffraction peak at $2\theta = 34.1°$, which is the crystal surface of Ni-phyllosilicate (111), reflecting the growth on the surface of SiO_2. After reduction, the diffraction peak was observed at $2\theta = 44.6°$ and 52.0° in all the catalysts, which is considered to be the diffraction peak of Ni (111) and (200), and the corresponding peak of Ni on catalyst Ni/V-SiO_2 is weaker than that on Ni/V-SiO_2-IM. The results show that the average particle sizes of Ni particles calculated by Scherrer equation are of 8.3 nm and 14.4 nm, which shows that the catalyst Ni/V-SiO_2 obtained smaller particle size by H_2 reduction.

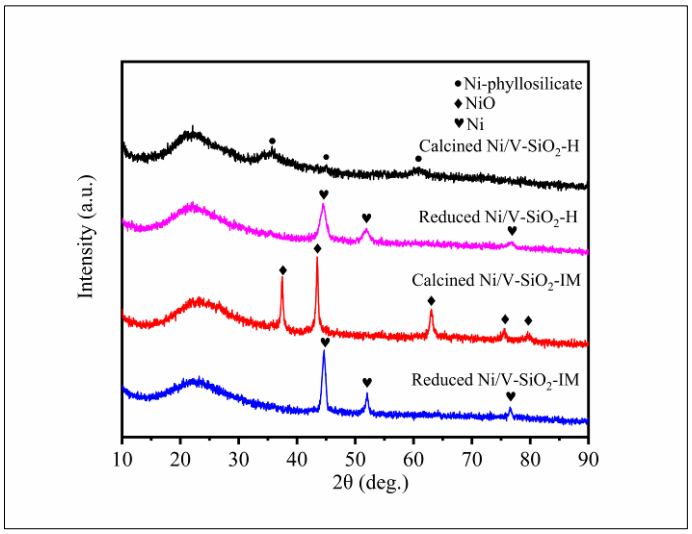

Figure 2. XRD patterns of the Ni/V-SiO_2-IM and Ni/V-SiO_2-H catalysts

3.3. XPS analysis

As for the further understanding of the composition and chemical state of the surface elements on the calcined catalyst, XPS characterization was performed (Figure 3), and there were great differences in the binding energy of the catalyst spectrum. The spectrum of Ni $2p_{3/2}$ was exhibited in Figure 3(a), the Ni $2p_{3/2}$ peak binding energy of calcined Ni/V-SiO_2-H was 857.28 eV, while the Ni $2p_{3/2}$ peak binding energy of Ni/V-SiO_2-IM was 855.18 eV and the peak intensity was weaker. According to the report of Lu et al. [30] the peak of Ni/V-SiO_2-IM at 855.18 eV could be considered as NiO species. For Ni/V-SiO_2-H, the peak binding energy of Ni $2p_{3/2}$ was shifted to 857.28 eV. Besides, in Figure 3(b), the Si 2p binding energy of Ni/V-SiO_2-H (103.48 eV) was lower than that of Ni/V-SiO_2-H (103.78 eV). The change of the binding energy of Ni and Si indicates the formation of Ni-phyllosilicate and the interaction between Ni and SiO_2 [31].

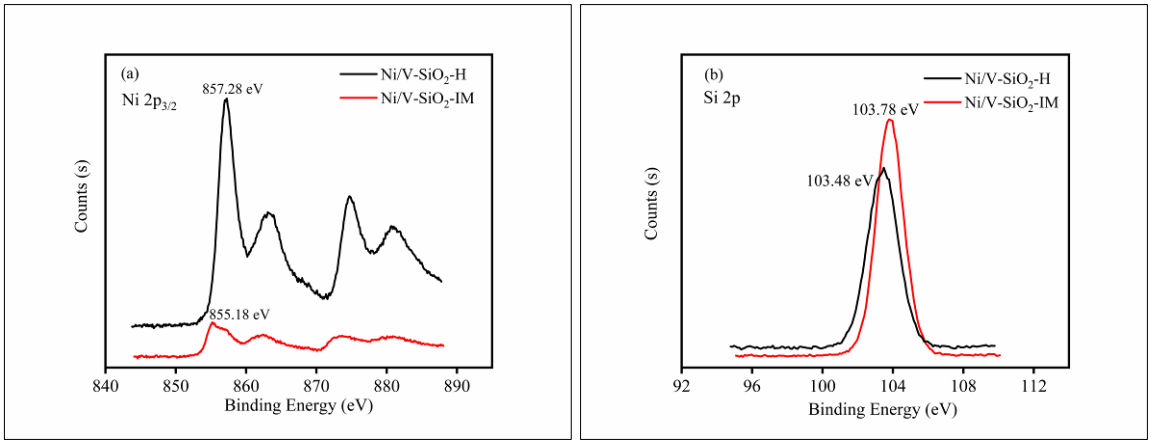

Figure 3. XPS Ni $2p_{3/2}$ (a) and Si 2p (b) spectra of the calcined Ni/V-SiO_2 samples

3.4. H_2-TPR analyses

To investigate the reduction performance of the catalyst, the H_2-TPR profiles of the Ni/V-SiO_2 sample were displayed in Figure 4. The peak at 299 and 381°C for Ni/V-SiO_2-IM is related to the reduction of NiO on the support surface [34], and the metal support interaction is relatively weak. Moreover, the shoulder reduction peaks at 564°C could be assigned to the reduction of nickel species

moderately interacted with support [35]. As for the profile of Ni/V-SiO_2-H, there is a broad peak at 703°C, while there is almost no obvious reduction peak at other positions, showing stronger interaction, which also implies that there is basically no NiO species in the catalyst. It is worth mentioning that this material may be Ni-phyllosilicate, which is difficult to reduce. Generally, it is determined that the enhancement of interaction between metal and support is determined by the increase in the reduction temperature [36]. After reduction, Ni particles were confined to SiO_2 support due to the strong interaction. The species of Ni-phyllosilicate played a significant role in improving the stability of Ni particles at high temperature.

3.5. Activity test results

Figure 5 shows the DRM catalytic performance of all catalysts. The initial CH_4 and CO_2 conversion of Ni/V-SiO_2-H catalyst were 71.7% and 80.2%, respectively. After 8 h of testing, the activity of the catalyst decreased slightly to 70.2% and 78.2%, and the H_2/CO ratio remained relatively stable. On the contrary, the activity of Ni/V-SiO_2-IM has been significantly decreased during the test period and showed severe deactivation. The conversion of CH_4 decreased from 67.5% to 61.7%, and the conversion of CO_2 decreased from 76.5% to 72.1%. At the same time, the ratio of H_2/CO decreased with the increase in the reaction time, which means the side reaction became serious. According to the reports in the literature, the sintering and carbon deposition of Ni particles are closely related to the deactivation of catalyst [32-33], so it is suggested that the anti-sintering and anti-carbon deposition ability of Ni/V-SiO_2-H is stronger than that of Ni/V-SiO_2-IM.

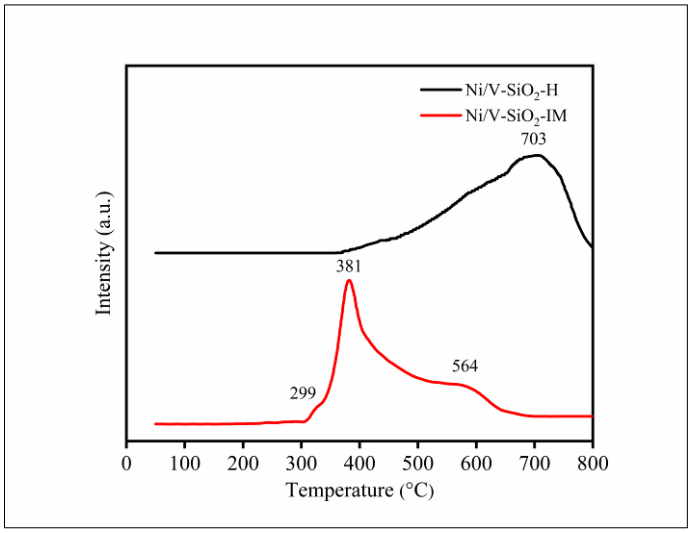

Figure 4. H_2-TPR profiles of calcined Ni/V-SiO_2-IM and Ni/V-SiO_2-H catalysts

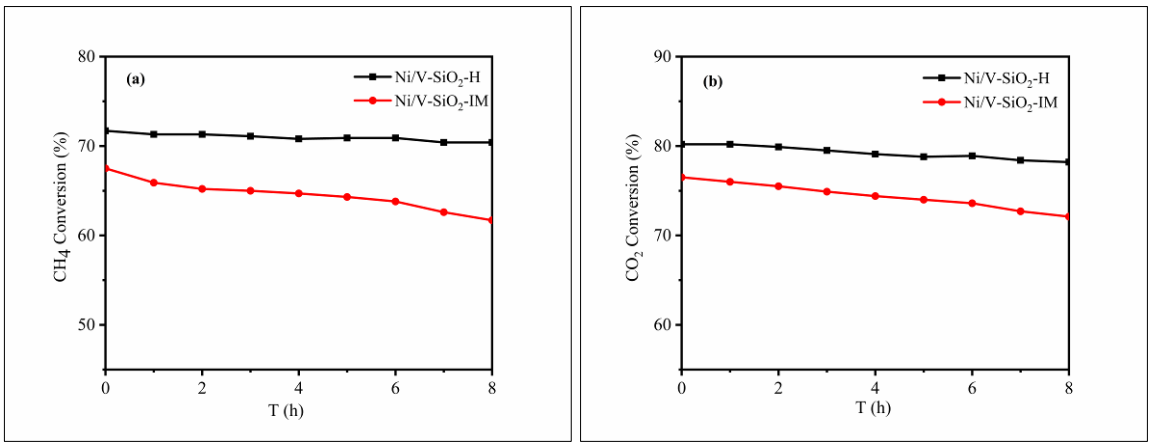

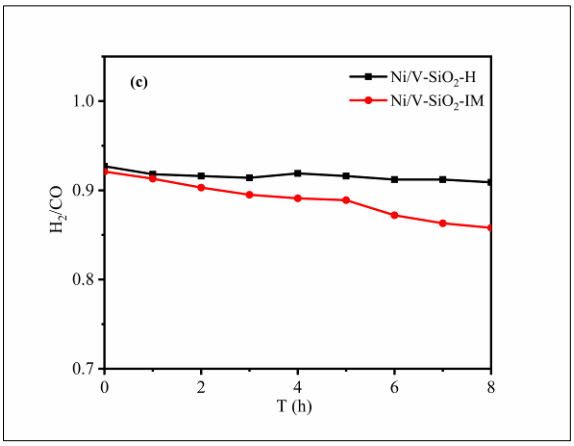

Figure 5. (a) CH_4 conversion, (b) CO_2 conversion, and (c) H_2/CO ratios of catalysts. (Reaction temperature = 700°C, GHSV = 18,000 mL h^{-1} g_{cat}^{-1})

3.6. XRD and analysis of spent catalysts

In order to further understand the change of catalyst after testing on stream, the catalyst were analyzed by XRD measurements. The XRD patterns of the spent catalyst were given in Figure 6. A new diffraction peak appeared at 2θ = 26.2° in the spent sample Ni/V-SiO_2-IM, indicating the existence of the peak of carbon species. However, the peak of carbon crystallization was not observed in Ni/V-SiO_2-H, which suggested that there was no or a small amount of carbon species. Furthermore, for all catalysts, the intensity of Ni diffraction peak was changed after testing compared with fresh catalyst. The average particle sizes of spent catalyst, which were calculated by Scheler equation, were of 11.3 nm and 17.5 nm, respectively.

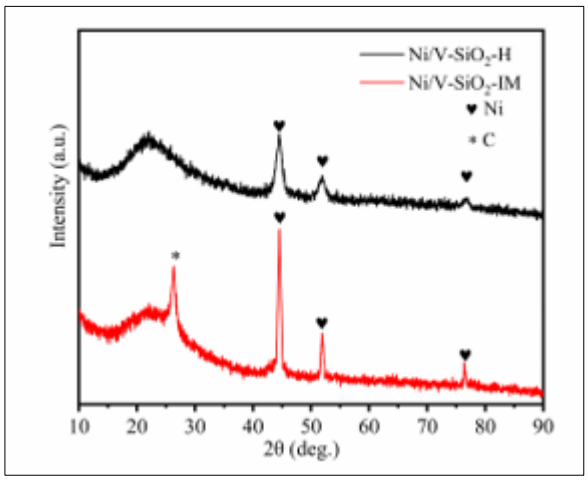

Figure 6. XRD patterns of the spent Ni/V-SiO_2-IM and Ni/V-SiO_2-H catalysts

3.7. TG analysis of the spent catalysts

In order to further understand the carbon deposition of the catalyst after the test, all samples were analyzed by thermogravimetry. The results given in Figure 7 show that at about 300°C, all the samples show weak weight loss, which is probably due to the elimination of amorphous carbon [37]. Another stage of weight loss at 500-700°C is attributed to the combustion of graphite phase carbon and carbon nanotubes [38]. The results show that the weight losses of Ni/V-SiO_2-IM and Ni/V-SiO_2-H at high temperature are of 26.8% and 5.4%, respectively, representing the excellent anti carbon deposition ability of Ni/V-SiO_2-H.

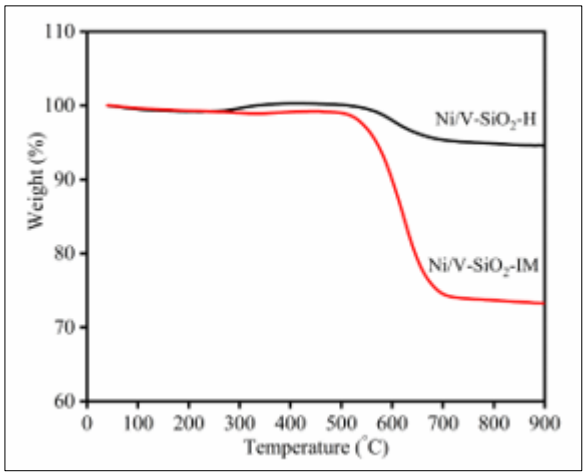

Figure 7. TG profiles of the catalysts after dry reforming of methane

3.8. TEM analysis of catalysts

The morphology and size distribution of Ni particles in reduced and spent Ni/V-SiO_2-H were characterized by TEM. In Figure 8(a), the nickel particles were dispersed homogeneously, with a very small portion of large nickel particles appearing, which was attributed to the reduction at high temperature. However, in Figure 8(b), it was found that there were more large nickel particles due to long-term high reaction temperature [39]. In addition, the formation of filamentous carbon deposited on the surface of spent catalyst was also shown, but from the test results, it seems that this did not significantly affect the catalytic activity. The particle size was dispersed in the range of 4-18 nm and increased to 6-22 nm after the reaction. Particle size distribution results were presented in Figure 8(c) and 8(d), after calculating that the average particle size of nickel particles was enlarged from 8.3 nm to 11.3 nm. Above all, the particle sizes of catalysts tested were almost consistent with the XRD results.

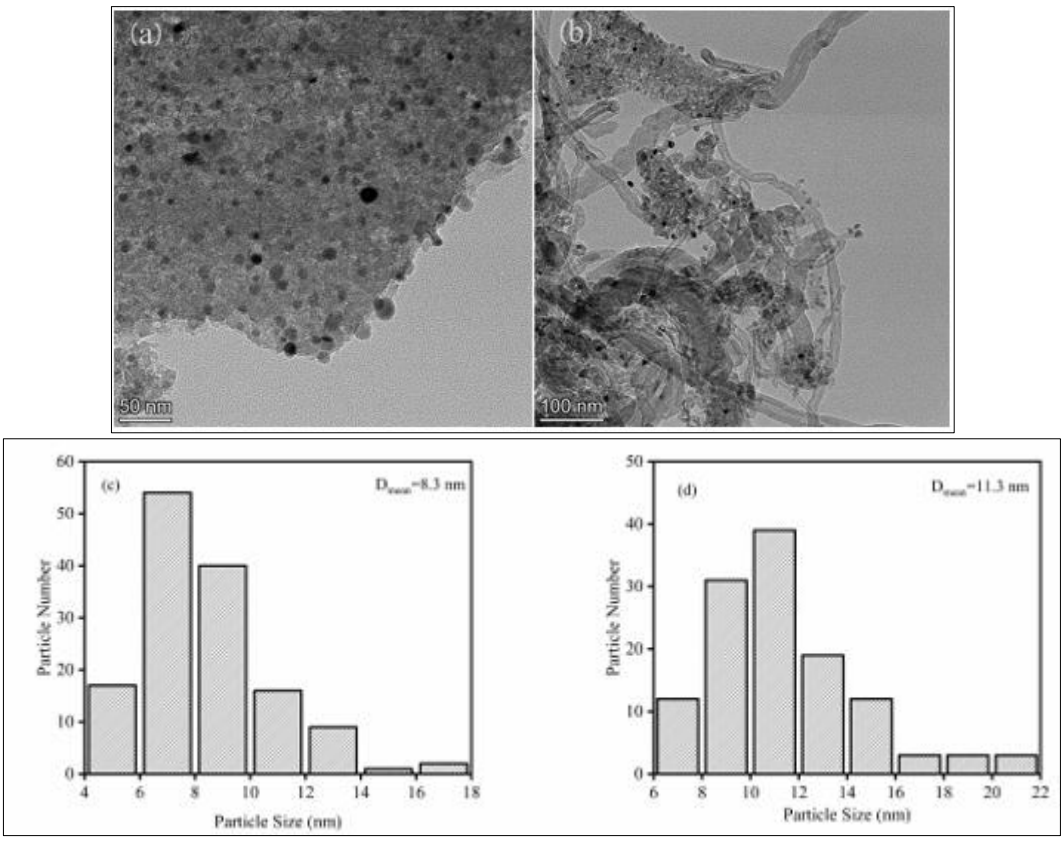

Figure 8. TEM images of Ni/V-SiO_2-H catalyst (a) after reduction (b) after testing, and Ni particle sizes distribution (c) after reduction (d) after testing

4. Conclusions

V-SiO_2 was successfully prepared from vermiculite by the method of mixed acid etching, and then used to prepare Ni-phyllosilicate. Compared with Ni/V-SiO_2-IM prepared by traditional impregnation method, Ni-phyllosilicate possessed smaller nickel particle size, higher dispersion and catalytic performance. The reason for these results was the strong metal support interaction of phyllosilicate. Therefore, SiO_2 derived from vermiculite and the preparation of Ni phyllosilicate have potential application prospects.

Acknowledgments: We are grateful for grants from Natural Science Foundation of China (NO 21766029), (NO 21566031) and Program of Science and Technology Innovation Team in Bingtuan (No.2020CB006).

References

1. JANG W J, SHIM J O, KIM H M, YOO S Y, ROH H S. A review on dry reforming of methane in aspect of catalytic properties [J]. Catalysis Today, 2018, 324: 15-26.
2. MARKEWITZ P, KUCKSHINRICHS W, LEITNER W, et al. Worldwide innovations in the development of carbon capture technologies and the utilization of CO_2[J]. Energy & Environmental Science, 2012, 5: 7281-7305.
3. WANG F, ZHANG L, XU L, DENG Z, SHI W. Low temperature CO oxidation and CH_4 combustion over Co_3O_4 nanosheets[J]. Fuel, 2017, 203: 419-429.
4. DING S, LIU Y. Adsorption of CO_2 from flue gas by novel seaweed-based KOH-activated porous[J]. Fuel, 2020, 260: 116382.
5. BIAN Z, DAS S, WAI M H, HONGMANOROM P, KAWI S. A Review on Bimetallic Nickel-Based Catalysts for CO_2 Reforming of Methane[J]. ChemPhysChem, 2017, 18(22): 3117-3134.
6. YABE T, SEKINE Y, Methane conversion using carbon dioxide as an oxidizing agent: A review[J]. Fuel Processing Technology, 2018, 181: 187-198.
7. GAO Y, JIANG J, MENG Y, YAN F, AIHEMAITI A. A review of recent developments in hydrogen production via biogas dry reforming[J]. Energy Conversion and Management, 2018, 171: 133-155.
8. NIKOO M, AMIN N. Thermodynamic analysis of carbon dioxide reforming of methane in view of solid carbon formation[J]. Fuel Processing Technology, 2011, 92(3): 678-691.
9. UCHIDA T, IKEDA I, TAKEYA S, et al. Kinetics and stability of CH_4-CO_2 mixed gas hydrates during formation and long-term storage[J]. ChemPhysChem, 2010, 6(4): 646-654.
10. LEE J H, YOU Y W, AHN H C, et al. The deactivation study of Co–Ru–Zr catalyst depending on supports in the dry reforming of carbon dioxide[J]. Journal of Industrial & Engineering Chemistry, 2014, 20(1): 284-289.
11.SINGH R, DHIR A, MOHAPATRA S K, MAHLA S K. Dry reforming of methane using various catalysts in the process: review[J]. Biomass Conversion and Biorefinery, 2020, 10: 567-587.
12.MOFRAD B D, REZAEI M, HAYATI-ASHTIANI M. Preparation and characterization of Ni catalysts supported on pillared nanoporous bentonite powders for dry reforming reaction[J]. International Journal of Hydrogen Energy, 2019, 44(50): 27429-27444.
13.NEMATOLLAHI B, REZAEI M, ASGHARI M, et al. A comparative study between modeling and experimental results over rhodium supported catalyst in dry reforming reaction[J]. Fuel, 2014, 134: 565-572.
14.TANKOV I, ARISHTIROVA K, BUENO J, DAMYANOVA S. Surface and structural features of Pt/PrO_2-Al_2O_3 catalysts for dry methane reforming[J]. Applied Catalysis A: General, 2014, 474: 135-148.
15.DOGHACHI F, RASHID U, ZAINAL Z, et al. Influence of Ce_2O_3 and CeO_2 promoters on Pd/MgO catalysts in the dry-reforming of methane[J]. RSC Advances, 2015, 5: 81739-81752.
16.SEO H O. Recent Scientific Progress on Developing Supported Ni Catalysts for Dry (CO_2) Reforming of Methane [J]. Catalysts, 2018, 8(3): 110.

17.ABDULLAH B, ABD GHANI N A, VO D V. Recent advances in dry reforming of methane over Ni-based catalysts [J]. Journal of Cleaner Production, 2017, 162: 170-185.
18.ZHANG G, LIU J, XU Y, SUN Y. A review of CH_4-CO_2 reforming to synthesis gas over Ni-based catalysts in recent years (2010-2017)[J]. International Journal of Hydrogen Energy, 2018, 43: 15030-15054.
19.QIN Z, CHEN J, XIE X, LUO X, JI H. CO_2 reforming of CH_4 to syngas over nickel-based catalysts[J]. Environmental Chemistry Letters, 2020, 18: 997-1017.
20.PARK J, YEO S, CHANG T. Effect of supports on the performance of Co-based catalysts in methane dry reforming [J]. Journal of CO_2 Utilization, 2018, 26: 465-475.
21.POMPEO F, NICHIO N N, FERRETTI O A, RESASCO D. Study of Ni catalysts on different supports to obtain synthesis gas[J]. International Journal of Hydrogen Energy, 2005, 30: 1399-1405.
22.HUANG F, WANG R, YANG C, et al. Catalytic performances of Ni/mesoporous SiO_2 catalysts for dry reforming of methane to hydrogen[J]. Journal of Energy Chemistry, 2016, 25: 709-719.
23.WANG L, WANG X, YIN J, WANG C. Insights into the physicochemical characteristics from vermiculite to silica nanosheets[J]. Applied Clay Science, 2016, 132-133: 17-23.
24.LI P, ZHU M, DAN J, et al. Two-dimensional porous SiO_2 nanomesh supported high dispersed Ni nanoparticles for CO methanation[J]. Chemical Engineering Journal, 2017, 326: 774-780.
25.YANG M, JIN P, FAN Y, et al. Ammonia-assisted synthesis towards a phyllosilicate-derived highly-dispersed and long-lived Ni/SiO_2 catalyst[J]. Catalysis Science & Technology, 2015, 5: 5095-5099.
26.BIAN Z, KAWI S. Preparation, characterization and catalytic application of phyllosilicate: A review[J]. Catalysis Today, 2020, 339: 3-23.
27.ZHANG Q, TANG T, WANG J, et al. Facile template-free synthesis of Ni-SiO_2 catalyst with excellent sintering- and coking-resistance for dry reforming of methane[J]. Catalysis Communications, 2019, 131: 105782.
28.DAN J, HUANG X, LI P, et al. Two-Dimensional Porous Silica Nanomesh from Expanded Multilayered Vermiculite via Mixed Acid Leaching[J]. Nanoscience and Nanotechnology Letters, 2016, 8: 1028-1032.
29.WANG S, WANG Y, HU C. The effect of $NH_3 \cdot H_2O$ addition in Ni/SBA-15 catalyst preparation on its performance for carbon dioxide reforming of methane to produce H_2[J]. International Journal of Hydrogen Energy, 2018, 43: 13921-13930.
30.LU B, JU Y, ABE T, KAWAMOTO K. Grafting Ni particles onto SBA-15, and their enhanced performance for CO_2 methanation[J]. RSC Advances, 2015, 5: 56444-56454.
31.WANG Z, XU Z, PENG S, et al. High-Performance and Long-Lived Cu/SiO_2 Nanocatalyst for CO_2 Hydrogenation[J]. ACS Catalysis, 2015, 5: 4255-4259.
32.SCHULZ L A, KAHLE L C, DELGADO K H, et al. On the coke deposition in dry reforming of methane at elevated pressures[J]. Applied Catalysis A: General, 2015, 504: 599-607.
33.TAHERIAN Z, YOUSEFPOUR M, TAJALLY M, KHOSHANDAM B. Promotional effect of samarium on the activity and stability of Ni-SBA-15 catalysts in dry reforming of methane[J]. Micro-porous and Mesoporous Materials, 2017, 251: 9-18.
34.CIOTONEA C, DRAGOI B, UNGUREANU A, et al. Nanosized transition metals in controlled environments of phyllosilicate-mesoporous silica composites as highly thermostable and active catalysts[J]. Chemical Communications, 2013, 49: 7665-7667.
35.HE S, JING Q, YU W, et al. Combination of CO_2 reforming and partial oxidation of methane to produce syngas over Ni/SiO_2 prepared with nickel citrate precursor[J]. Catalysis Today, 2009, 148: 130-133.
36.ASHOK J, BIAN Z, WANG Z, KAWI S. Ni-phyllosilicate structure derived Ni-SiO_2-MgO catalysts for bi-reforming applications: acidity, basicity and thermal stability[J]. Catalysis Science & Technology, 2018, 8: 1730-1742.

37.ZHANG Q, WANG J, NING P, et al. Dry reforming of methane over Ni/SBA-15 catalysts prepared by homogeneous precipitation method[J]. Korean Journal of Chemical Engineering, 2017, 34: 2823-2831.
38.FANG X, ZHANG X, GUO Y, et al. Highly active and stable Ni/$Y_2Zr_2O_7$ catalysts for methane steam reforming: On the nature and effective preparation method of the pyrochlore support[J]. International Journal of Hydrogen Energy, 2016, 41: 11141-11153.
39.ARORA S., PRASAD R., An overview on dry reforming of methane: strategies to reduce carbonaceous deactivation of catalysts[J]. RSC Advances, 2016, 6: 108668-108688

Manuscript received: 24.04.2021